

# Università degli Studi di Catania Scuola Superiore di Catania

---

International PhD  
in  
STEM CELLS  
XXIII cycle

Therapeutic effect of adipose tissue-mesenchymal stem cells  
transplantation in rats with acute liver failure

FEDERICO SALAMONE

*A.A. 2009/2010*

Coordinator of PhD  
Prof. Daniele Condorelli

Tutor  
Prof. Lidia Puzzo

## **BACKGROUND AND AIMS**

Mesenchymal Stem Cells (MSCs) are adherent, fibroblast-like, pluripotent and non-hematopoietic progenitor cells, which reside in most organs investigated so far including bone marrow<sup>1</sup>, umbilical cord<sup>2</sup>, amniotic fluid<sup>3</sup>, placenta<sup>4</sup> and subcutaneous adipose tissues<sup>5-7</sup>. They display the capacity to differentiate *in vitro* into multiple mesodermal and non-mesodermal tissues. Most evidences regard bone marrow-derived mesenchymal stem cells (BM-MSCs) which can undergo chondrogenic<sup>1</sup>, osteogenic<sup>1</sup>, adipogenic<sup>1</sup>, myogenic<sup>8</sup> and even neurogenic<sup>9</sup> differentiation.

BM-MSCs can also differentiate in hepatocyte-like cells using an appropriate hepatogenic medium *in vitro*<sup>10</sup> and these BM-derived cells are also able to engraft in the liver of mice with experimental liver failure<sup>11</sup>. The hepatogenic potential of BM-MSCs has been confirmed in a number of experimental models of liver injury, suggesting that BM-MSCs can be considered as a possible source of hepatocyte-like cells of clinical interest. Nonetheless, the need of an invasive procedure for the isolation of BM-MSCs and the limited quantity of cells obtained from bone marrow aspirates makes the use of BM-MSCs not reliable in clinical practice. The search for novel cell resources has prompted investigations into isolating MSCs

from adipose tissue because of their ready availability and unrestricted potential to propagate and differentiate.

To this respect, adipose tissue mesenchymal stem cells (ASCs) are largely present in subcutaneous adipose tissue and thus can represent an easy source of MSCs also in patients with critical acute or chronic diseases using lipoaspiration. It has been elegantly showed<sup>12</sup> that ASCs are superior to BM-MSCs and umbilical-MSCs in terms of colony frequency and show also higher proliferation capacity as compared to BM-MSCs. Furthermore, the hepatogenic differentiation of ASCs has been demonstrated *in vitro* and *in vivo*, using different protocols<sup>13,14</sup>.

Acute liver failure (ALF) is a life-threatening condition in which a sudden and massive liver injury caused by different noxae can lead to hepatic encephalopathy, coagulopathy and in many cases to multiorgan failure<sup>15</sup>. A variety of etiologies including drugs, viral infections, alcohol, metabolic, autoimmune or genetic disorders may cause acute hepatic dysfunction, determining liver failure leading to death. The main cause of ALF in industrialized countries is acetaminophen (APAP) intoxication<sup>15</sup>. Although APAP is a safe and widely used analgesic drug, APAP overdose can lead to ALF and the mortality for APAP-ALF is currently impressive<sup>15</sup>. Cerebral edema is the main pathophysiological factor leading to death in patients with ALF<sup>15</sup>. A number of studies in human and rodents suggest

that oxidative stress plays a key role in the pathogenesis of APAP-ALF<sup>16</sup>. Oxidative stress is the consequence of the acute depletion of GSH that occurs early, after 1.5-2 h from APAP overdose, and it's caused by the generation of N-acetyl-p-benzoquinone imine (NAPQI), the toxic metabolite of APAP<sup>15</sup>. This early event lead to an impaired defense of liver cells against Reactive oxygen species (ROS) and Reactive nitrogen species which are able to determine lipid and protein peroxidation and DNA oxidative damage with consequent death of hepatocytes<sup>16-19</sup>. Together with oxidative stress, JNK activation seem to play a major role in the pathogenesis of APAP-induced liver failure<sup>20-22</sup>.

The pharmacological treatment of APAP-ALF is based on the use of N-Acetyl-Cysteine (NAC)<sup>15</sup>. However, in a number of patients with APAP-ALF, pharmacological treatment fails and patients need to undergo orthotopic liver transplantation (OLT)<sup>15</sup>. However, the shortage of donor organs for OLT makes the need of finding alternative therapeutic options. In this study, we aimed at identifying if the transplantation of ASCs may exert a therapeutic effect in APAP-ALF. We also aimed at identifying the underlying molecular events of ASCs transplantation, with particular interest on oxidative stress, mitochondrial damage and JNK activation in the liver and brain of rats with APAP-induced ALF.



## MATERIALS AND METHODS

***ASCs isolation and culture.*** Subcutaneous adipose tissue was obtained from a 23-year-old man with no significant medical history undergoing umbilical hernioplasty. Written consent was obtained. The choice of a single young and healthy man as source of ASCs was in order to eliminate any bias related to the use of cells from different individuals, which can display different functional activity, and to exclude any situation of disease that could have affected the proliferative properties of ASCs. Adipose tissue was minced with scissors and scalpels into less than 3-mm pieces and isolation of AT-MSCs proceeded as previously described<sup>14</sup>. Briefly, after gentle shaking with equal volume of PBS, the mixture separated into two phases. The upper phase (containing stem cells, adipocytes and blood) after washing with phosphate-buffered saline (PBS) was enzymatically dissociated with 0.075% collagenase (type I)/PBS for 1 hour at 37°C with gentle shaking. The dissociated tissue was then mixed with an equal volume of DMEM (GIBCO-BRL, Tokyo, Japan) supplemented with 10% fetal bovine serum (FBS) and incubated 10 minutes at room temperature. The solution then was separated into two phases. The lower phase was centrifuged at 1,500rpm for 5 minutes at 20°C. The cellular pellet was resuspended in 160mM NH<sub>4</sub>Cl to eliminate erythrocytes and passed through a 40µm mesh filter into a new tube. The cells were resuspended in an equal volume

of DMEM/10% FBS and then centrifuged. Isolation resulted in obtaining  $7.7 \times 10^6$  of adherent cells for a primary culture from 5g of adipose tissue (approximately;  $1.0 \times 10^5$  to  $4.6 \times 10^6$ /1g) after 7-10 days of culture. The cells were suspended in a DMEM/10% FBS plated in concentration  $1-5 \times 10^6$  cells/75cm<sup>2</sup>. The cells with 70%-80% confluence were harvested with 0.25% trypsin-EDTA and then either re-plated at  $1.0 \times 10^5$  cells/60-mm dish and used for analysis or sorted using MACS system (Miltenyi Biotec., Bergisch Gladbach, Germany).

***Isolation of the CD105<sup>+</sup> fraction from ASCs.*** The CD105<sup>+</sup> fraction was isolated from undifferentiated ASCs of the donor using CD105-coupled magnetic microbeads (Miltenyi Biotec), as previously described. Briefly, trypsinized ASCs ( $0.5-1.0 \times 10^8$  cells) were suspended in a MACS buffer (PBS/0.5 bovine serum albumin/2mM EDTA) and incubated with antibodies (8°C, 15 minutes). After rinsing with the MACS buffer and centrifugation (200 x g, 10 minutes), the cells were separated on a magnetic column. After the separation, approximately  $2.0-8.0 \times 10^5$  CD105<sup>+</sup> cells were achieved, plated in 60mm dishes, expanded, and used for experimental analysis. ASCs were transplanted at passage #5.

***Flow Cytometry.*** The phenotype of ASCs was evaluated by flow cytometry analysis (FACS, Epic XL, Software Expo 32 (Beckman coulter), by using CD29 (BD Bioscience Pharmingen, Tokyo, Japan), CD31, CD45 (eBioscience, Tokyo,

Japan), CD34 (DacoCytomation, Carpinteria, USA) and CD105 (Ancell, Bayport, MN, USA) antibodies, coupled to either phycoerythrin (PE) or fluorescein isothiocyanate (FITC).

***Green Fluorescent Protein (GFP) transfection of ASCs.*** Before transplantation cells were transfected with a baculovirus-mediated transfection system for GFP (Invitrogen, US), following manufacturer's instructions.

***Animals and treatments.*** Sprague-Dawley female rats were purchased from Charles River Lab (Calco, Italy). Animals were maintained in a light- and temperature- controlled facility and fed standard chow and water ad libitum. After an overnight fast, twelve rats weighting about 200 gr were administrated a 300 g/Kg body weight dose of APAP (Sigma, Italy) dissolved in PBS. After 1.5-2 hours from APAP administration, six rats received the infusion via the caudal vein of 200.000 cells suspended in 1 ml of saline; six rats were administrated only saline. Four rats were administrated only the vehicles and served as healthy control. After 24 hours from APAP administration, rats were sacrificed by cardiac puncture; blood, liver and brain were harvested for further analysis.

***Plasma biochemical analysis.*** Plasma levels of glucose, AST, ALT, bilirubin, ammonia and protrombin time were determined on blood samples using a Cobas

Multi-analyzer (Roche Diagnostics, UK) using appropriate kits and following standard procedures.

***Histology, immunofluorescence and immunohistochemistry.*** Liver samples were fixed in 10% buffered formalin and embedded in paraffin using standard techniques. Histological damage was evaluated by using hematoxylin-eosin staining. Indirect immunofluorescence for the identification of GFP<sup>+</sup> cells was performed on frozen liver samples. Monoclonal antibodies for human CK-8, pankeratin AE1/AE3,  $\alpha$ -SMA, desmin, vimentin, GFAP and CD105 (all from DakoCytomation, Italy) were used on paraffin-embedded sections, following manufacturer's instructions. All antibodies did not cross-react with rat proteins, as we evidenced in previous experiments.

***Brain edema measurement.*** Brain water content was determined by the wet/dry weight method. Approximately 10 mg tissue (three to four pieces from each animal) of cerebral cortex was dissected; wet weights of tissue were determined; tissue was dried overnight in an oven at 120°C; and dry weights determined. The difference in wet/dry weights was expressed as percent water content.

### **Liver oxidative stress meseasurements.**

Liver isoprostanes and 8-hydroxyguanosine (8-OHG) were determined by enzyme-linked immunosorbent assay (ELISA) test (Cayman, Ann Arbor, Michigan), following manufacturer's instructions. Data were expressed as pg/mL. Nitrite, the stable metabolite of nitric oxide, was measured colorimetrically *via* Griess reaction. Aliquots of homogenates were preincubated for 30 min at room temperature with 50  $\mu$ M nicotinamide adenine dinucleotide phosphate (Sigma) and 24 mU nitrate reductase (Roche Diagnostics GmbH, Mannheim, Germany), and then the samples were treated with 0.2 U lactate dehydrogenase (Roche) and 0.5  $\mu$ mol sodium pyruvate for 10 min. The coloration was developed adding Griess reagent (Merck KGaA, Darmstadt, Germany; 1:1, vol/vol). Finally, after 10 min at room temperature, absorbance was recorded by 96-well plate microtiter (Thermo Labsystems Multiskan, Milford, MA) at  $\lambda = 540$  nm. Nitrite levels were determined using a standard curve and expressed as nanomoles of nitrite/nitrate per milligram of protein. Protein content was determined by Bredford assay.

### **Western blot analysis for hepatic JNK**

Whole liver homogenates were processed for Western blot analysis and protein levels were visualized by immunoblotting with antibodies against the total JNK and pospho-JNK (Upstate, St. Charles, Missouri). Briefly, 30  $\mu$ g proteins were

separated by sodium dodecyl sulfate–polyacrylamide gel electrophoresis and transferred to a nitrocellulose membrane (Amersham Inc., Piscataway, NJ) using a semidry transfer apparatus (Bio-Rad, Hercules, CA). Membranes were incubated with a 1:1.000 dilution of specific antibody overnight with constant shaking. The filters were then washed and subsequently probed with Goat anti-rabbit antibodies labeled with IRDye 680 (1:10.000 dilution, LI-COR Biosciences, Lincoln, NE) and hybridization signals were detected with the Odyssey Infrared Imaging System (LI-COR Biosciences). Densitometric analysis was then performed and normalized with relative actin (Chemicon).

### **Statistical analysis**

Statistical analysis was aided by the SPSS Statistical Software for Windows, version 9 (SPSS Inc., Chicago, IL). The unpaired t test was used to assess the significance of differences between means. All results were expressed as mean  $\pm$  SD unless otherwise mentioned. P values less than 0.05 were considered significant.

## RESULTS

### Effects of ASCs transplanted on plasma AST and ALT levels.

Rats treated with 300 mg/Kg of APAP presented a two-fold increase in plasma levels of AST ( $P<0.01$ ) as compared with control healthy animals. Interestingly, rats transplanted with ASCs had AST levels not only lower than APAP-treated animals ( $P<0.01$ ) but also lower than the control group ( $P<0.05$ ).

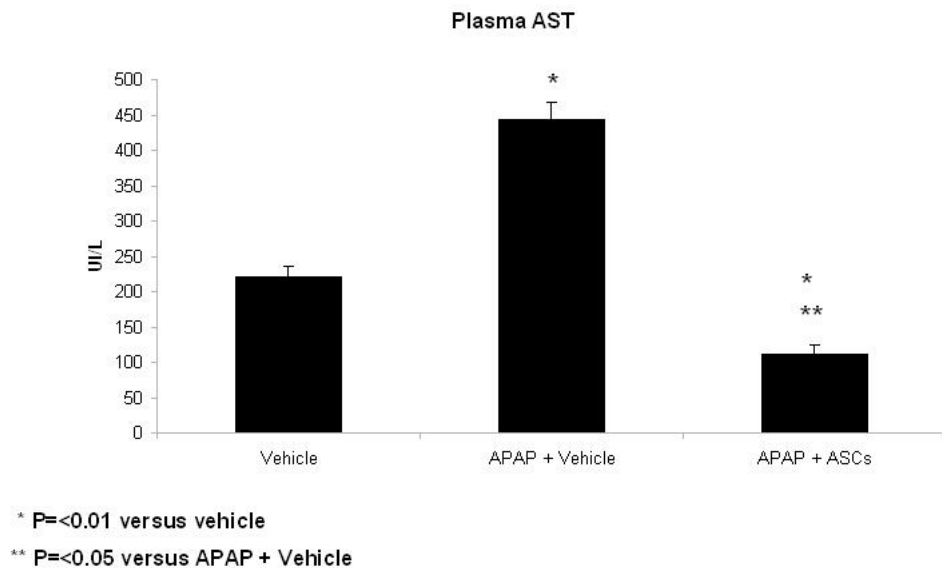
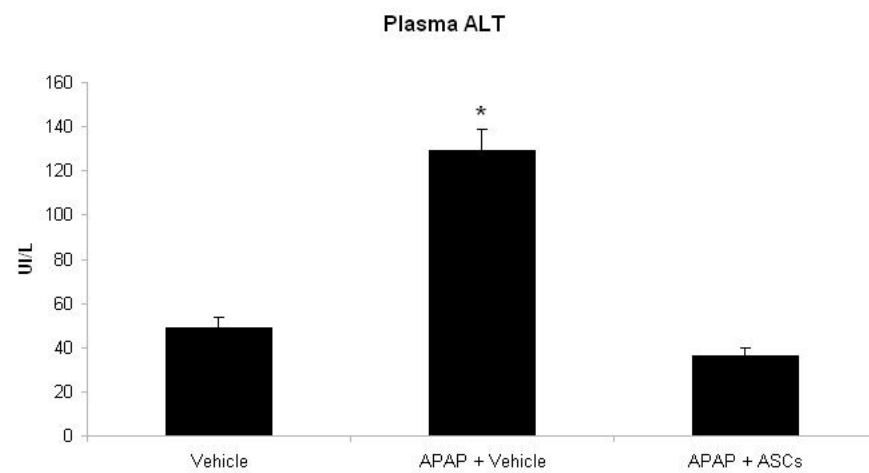


FIGURE 1. *AST levels*

Similarly, rats treated with 300 mg/Kg of APAP presented a marked increase in the activity of ALT as compared with control healthy animals ( $P<0.01$ ), indicating significant necrotic injury of hepatocytes. Rats transplanted with ASCs had ALT levels not only lower than APAP-treated animals ( $P<0.01$ ) but also lower than the control group ( $P<0.05$ ).



\*  $P<0.01$  versus vehicle

FIGURE 2. *ALT levels*



### Effect of ASCs transplantation on plasma ammonia and brain edema.

Consistently with the clinical evidence of encephalopathy, rats treated with APAP had higher levels of plasma ammonia than healthy controls ( $P<0.05$ ). On the contrary, in animals transplanted with ASCs ammonia levels were similar to those observed in the control group.

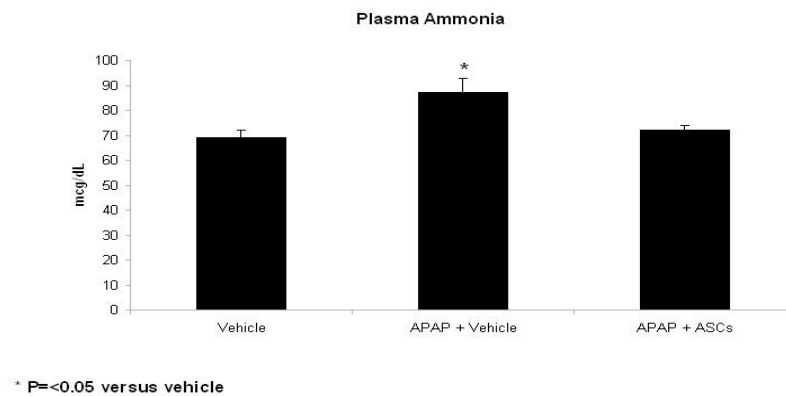


FIGURE 3. *Ammonia levels*

Consistently with clinical encephalopathy and plasma ammonia measurement, rats with APAP-induced ALF presented increased levels of brain water content as compared to control rats ( $P<0.05$ ), indicating failure of liver detoxifying pathways leading to brain edema. Strikingly, in animals transplanted with ASCs brain water content was comparable to the control group.

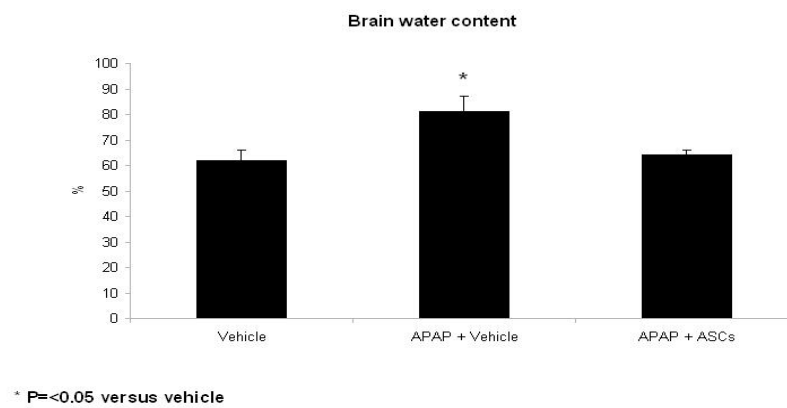


FIGURE 4. *Brain water content*

### Effect of ASCs transplantation on Prothrombin Time (INR)

Rats treated with 300 mg/Kg of APAP presented a two-fold increase in Prothrombin Time as compared with control healthy animals ( $P<0.01$ ), thus indicating failure of liver protidosynthetic function in intoxicated animals. In rats transplanted with ASCs, INR levels were restored to the levels observed in the control group.

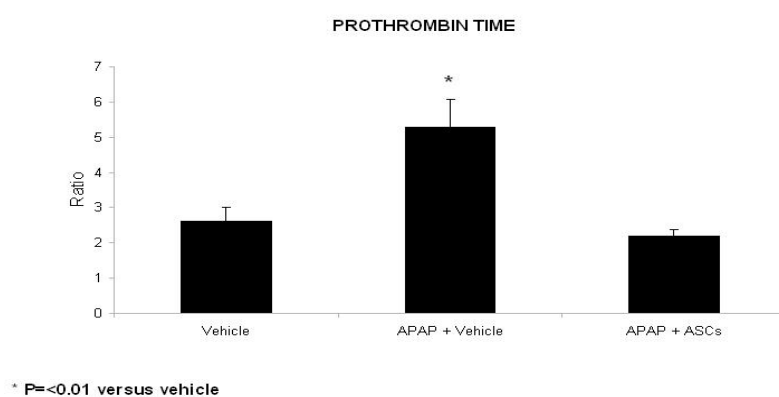


FIGURE 5. *Prothrombin time*

### **Effect of ASCs transplantation on liver histology.**

Rats treated with 300 mg/Kg of APAP presented diffused vacuolar degeneration due to mitochondrial and endoplasmic reticulum injury; necroinflammatory foci were both present in the portal and lobular area.

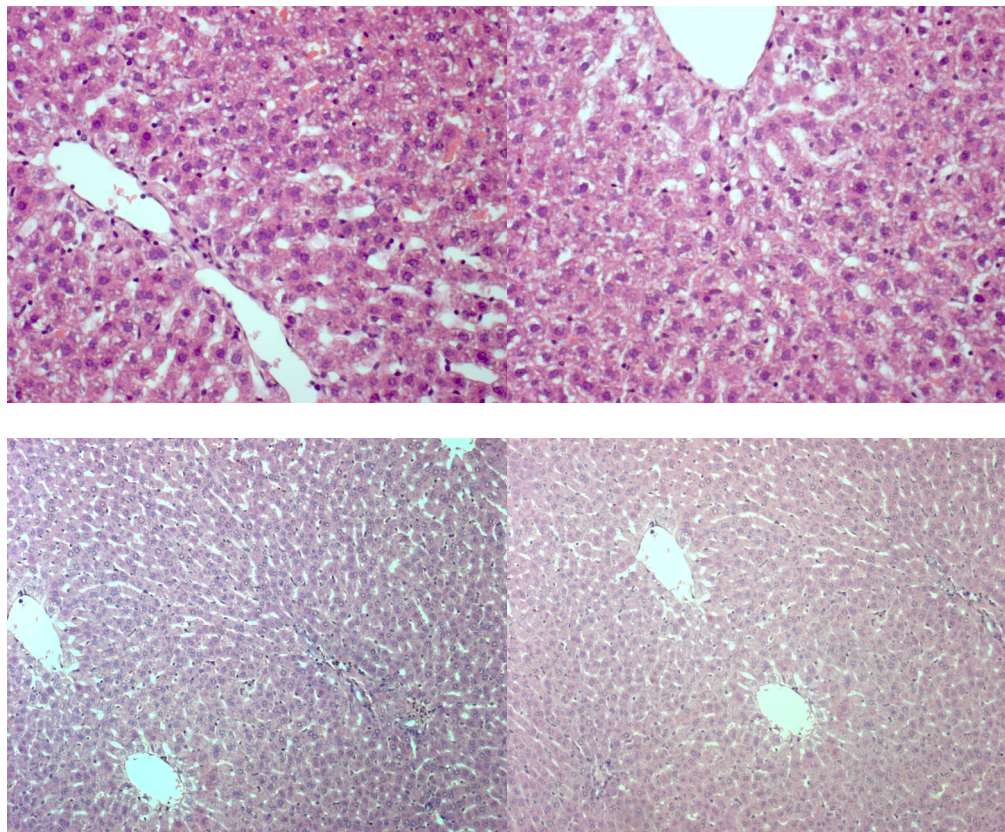


FIGURE 6. *Liver sections of rats with APAP-induced liver injury (A, B. 40x) and liver sections of healthy control rats (C, D. 10x).*

In rats transplanted with ASCs, no sign of necroinflammation was present and only mild vacuolar degeneration was focally observed.

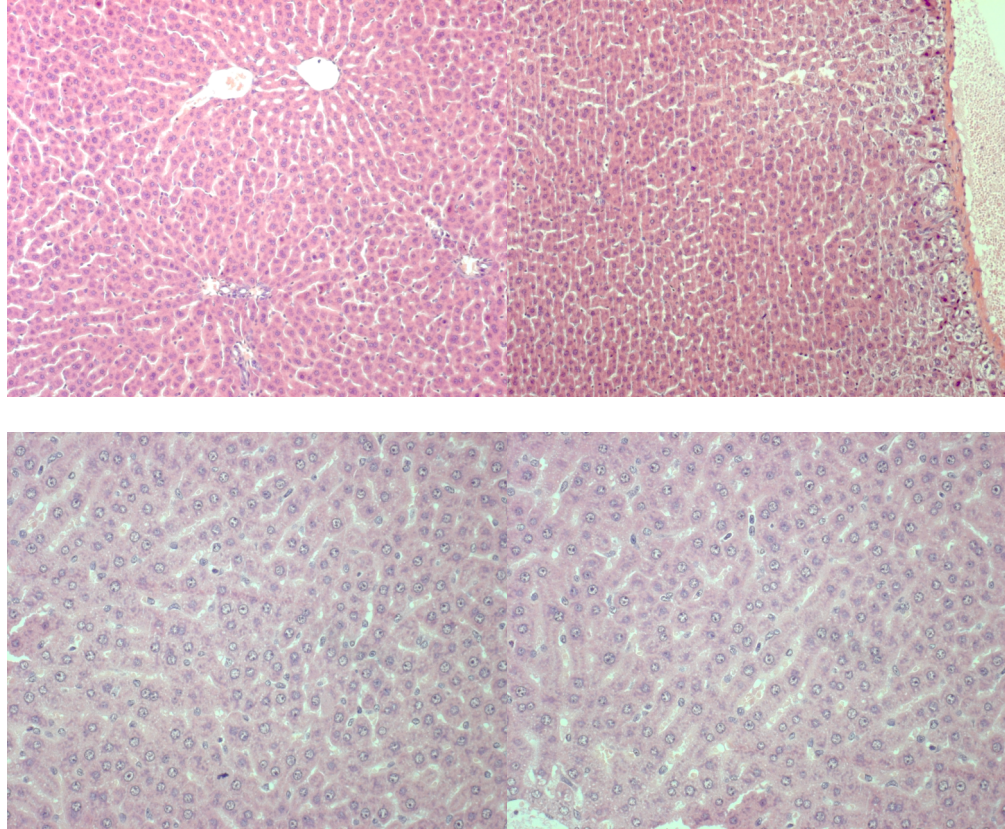


FIGURE 7. *Liver sections of rats with APAP-induced liver injury and transplanted with ASCs [magnification: (A, B. 10x) (C, D. 40x)]*



In several liver sections of rats transplanted with ASCs, mitotic hepatocytes were diffusely present while these were almost absent in control rats.

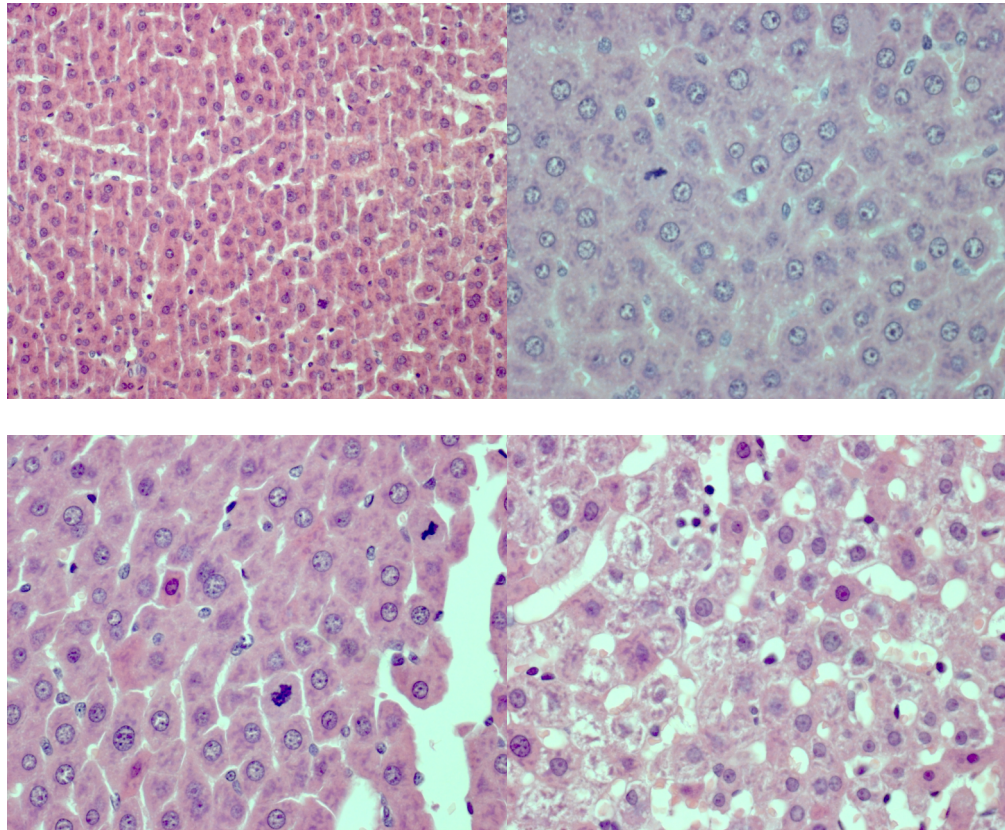


FIGURE 8. *Liver sections of rats with APAP-induced liver injury and transplanted with ASCs [magnification: (A, B. 10x) (C, D. 40x)]*

### **Liver engraftment and ASCs immunophenotype/morphology**

Immunofluorescence for GFP revealed the presence of ASCs in almost all liver sections of transplanted rats, indicating that ASCs exerted liver protection by acting locally although it is not possible to exclude different organ localization. In most sections, ASCs presented shaped fibroblast-like morphology and localized around sinusoids which are a main target of APAP hepatotoxicity.

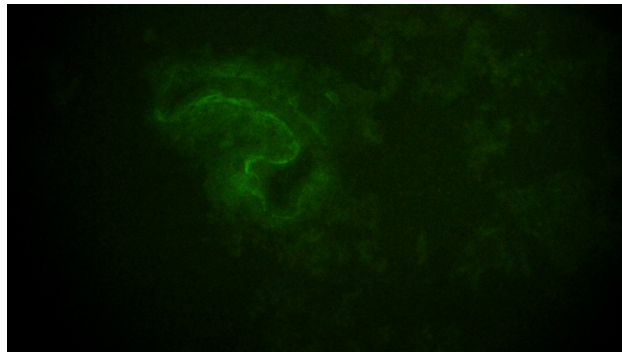


FIGURE 9. *Liver sections of rats with APAP-induced liver injury and transplanted with ASCs [magnification: 10x]*

In few liver sections, ASCs appeared with a round epithelial-like morphology, suggesting that a proportion of ASCs undergo hepatocyte differentiation in vivo.

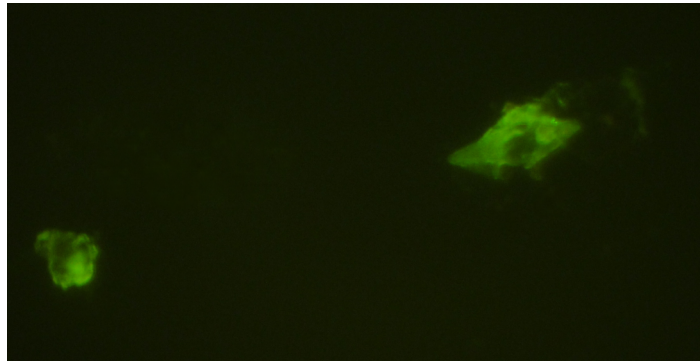


FIGURE 10. *Liver sections of rats with APAP-induced liver injury and transplanted with ASCs [magnification: 40x]*

Immunohistochemistry with monoclonal antibodies against CK-8 confirmed the presence of few ASCs which are differentiating in hepatocytes, whereas in almost all liver sections of transplanted rats, ASCs were vimentin-positive.



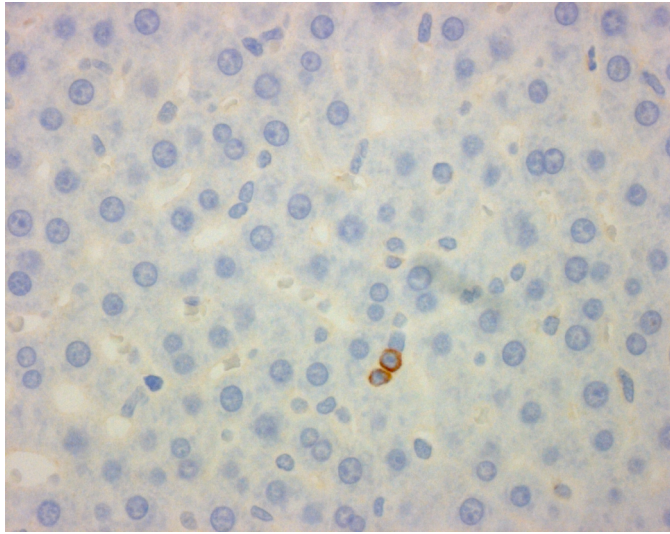


FIGURE 11. *Immunohistochemistry for human CK-8 (40x)*

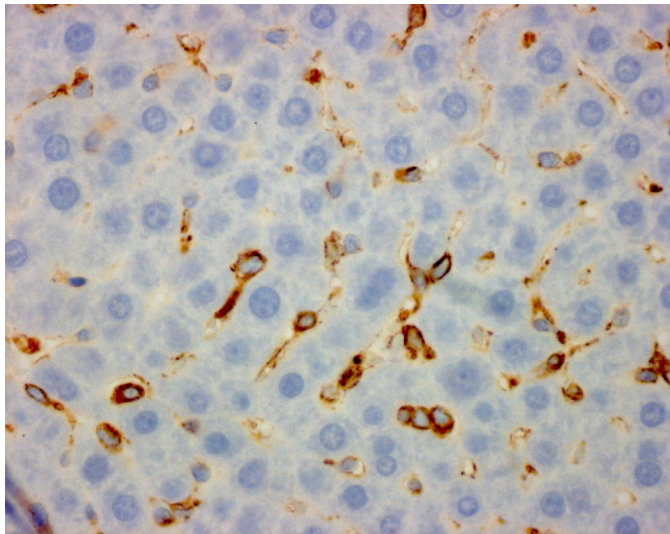


FIGURE 12. *Immunohistochemistry for human vimentin (40x)*

### Effect of ASCs on liver oxidative stress.

Rats treated with 300 mg/Kg of APAP presented a three-fold increase in hepatic levels of isoprostanes ( $P<0.01$ ) as compared with control healthy animals. Interestingly, rats transplanted with ASCs had isoprostanes levels similar to the control group .

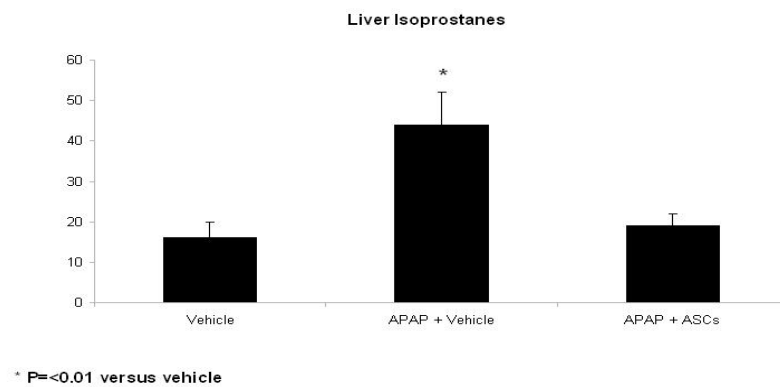


FIGURE 13. *Liver isoprostanes*

Similarly, rats treated with 300 mg/Kg of APAP presented a marked increase in liver 8-OHG as compared with control healthy animals ( $P<0.01$ ), indicating significant DNA damage of liver cells in intoxicated animals. Rats transplanted with ASCs had 8-OHG levels not different from the control group.

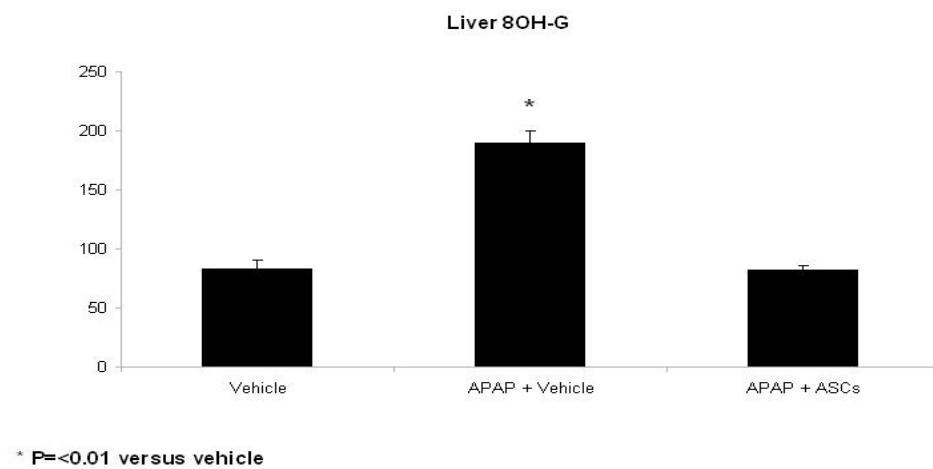


FIGURE 14. *Liver 8OHG*

Consistently with isoprostanes and 8-OHG values, rats with APAP-induced ALF presented increased levels of hepatic nitrite/nitrates as compared to control rats ( $P<0.01$ ), indicating nitrosative stress. Strikingly, in animals transplanted with ASCs, nitrite/nitrates were comparable to the control group.

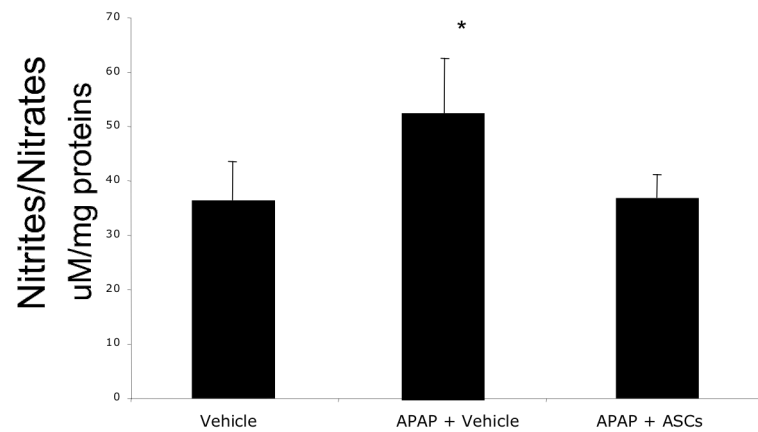


FIGURE 15. *Liver nitrite/nitrates*

### Effect of ASCs transplantation on liver JNK activation.

Rats treated with 300 mg/Kg of APAP presented an increase of phospho-JNK expression whereas the levels of total JNK were not significantly modified. In rats transplanted with ASCs, p-JNK expression was restored to the levels observed in the control group.

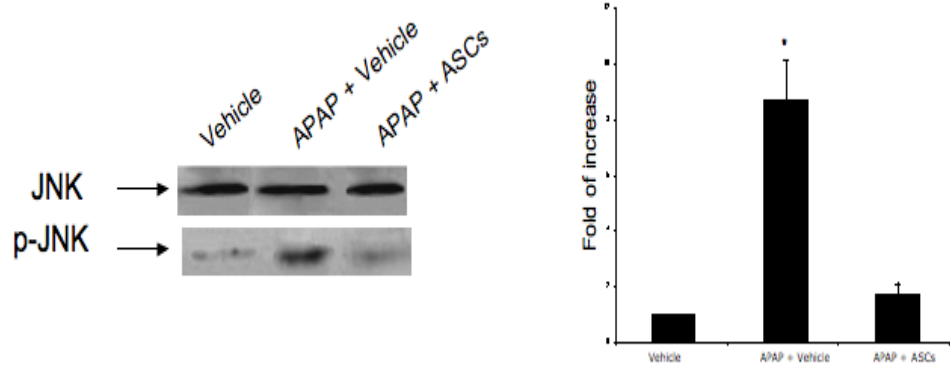


FIGURE 16. *Liver JNK expression*

## DISCUSSION

In the current study, we explored the effect of ASCs transplantation in rats with APAP-induced liver failure. APAP intoxication is the leading cause of ALF in industrialized countries and the mortality for APAP-ALF is currently high<sup>15</sup>. The shortage of grafts for OLT determines the need of novel therapies for ALF. Recent studies indicates that the transplantation of mature hepatocytes or hepatocyte-like cells derived from adult stem cell of various origin represent a promising tool for the treatment of chronic liver diseases<sup>23</sup>. However, in critical acute conditions as in APAP-induced ALF, it is mandatory to offer an immediate treatment, thus we choosed to evaluated the effect of ASCs transplantation and not ASCs-derived hepatocyte-like cells because the need for long-time period of culture makes the use unreliable in clinical practice in acute conditions. Furthermore, it has been showed<sup>24</sup> that in rats with CCl4-induced liver failure the transplantation of undifferentiated BM-MSCs is more effective for clinical rescue than the transplantation of hepatocyte-like cells derived from these cells; in particular, this effect was dependent on the greater resistance to oxidative stress of undifferentiated BM-MSCs as compared to BM-MSCs undergoing *in vitro* hepatogenic differentiation.

In the same direction, we choosed to use ASCs because of their ready availability and unrestricted potential to propagate and differentiate. Moreover, it has been recently showed<sup>25</sup> that undifferentiated ASCs express markers of adult hepatocytes, as CK-18 and albumin which are not expressed by BM-MSCs, indicating that these cells are in a state of differenation which is nearer to mature hepatocytes than BM-MSCs. To our knowledge, this is the first demonstration of the effectiveness on ASCs transplantation in experimental APAP-induced liver failure.

ASCs transplantation was effective on the whole spectrum of clinical and molecular abnormalities observed in rats with APAP-ALF. From a clinical point of view, ASCs transplantation completely counteracted the appearance of liver injury and encephalopathy. Transplanted animals had levels of transaminases, ammonia and PT comparable to those of healthy control rats and did not displayed either brain edema or any neurological abnormality. These findings are particularly relevant because the two main clinical features of ALF are coagulopathy and encephalopathy<sup>15</sup>. Clinical findings were consistent with histological data, which showed massive necrotic injury in vehicle-treated animals, whereas transplanted animals presented only mild injury. Interestingly, we did not observe any sign of reject. This is dependent on the lack of immunogenicity of MSCs and is consistent

with previous studies demonstrating immunotolerance of human MSCs in rodent models of liver injury<sup>11</sup>.

An important question regarded whether ASCs exerted a putative therapeutic effect in- or outside the liver and whether, in the case of engraftment in the host liver, ASCs maintained their fibroblast-like phenotype or underwent hepatogenic differentiation. GFP transfection allowed us to identify ASCs in the liver of rats, where they were present in different areas of the hepatic lobule and presented both a shaped morphology, typical of stromal cells, and an epithelial morphology in few cases. Interestingly, in many liver sections we observed ASCs localized around sinusoids. Endothelial sinusoidal cells damage is a key feature of APAP-induced ALF<sup>26</sup>; The maintenance of hepatic microcirculation in the presence of a toxic insult is critical to halt the progression of tissue damage. An accumulating body of evidence suggests that LSEC damage and disruption of the hepatic microcirculation represent key factors in the mechanisms of several models of liver injury<sup>27-29</sup>. In the pathogenesis of AILI, it has been demonstrated that damage to LSEC and impairment of hepatic microcirculation precede NAPQI-induced direct hepatocellular damage<sup>27,28</sup> and recent evidences suggests that the amelioration of LSEC injury can reduce the extent of AILI<sup>26</sup>. Thus, we can speculate that ASCs localized around sinusoidal cells because of chemotactic signals from endothelial



cells and target endothelial cell with trophic factors. These findings indicates a possible trophic activity of ASCs which is in agreement with previous data in mice treated with CCl<sub>4</sub> and tranplantated with ASCs<sup>30</sup>. Moreover, the production of trophic factors is considered a key feature of MSCs<sup>31</sup>. Moreover, in numerous sections of transplanted rats we observed mitotic hepatocytes, indicating that the therapeutic effect of ASCs is mainly dependent on a trophic activity towards hepatocytes and sinusoidal cells. Nonetheless, in few sections ASCs presented an epithelial morphology and expressed epithelial markers as CK-8; thus, it is not possible to exclude that in a longer period of observation ASCs can undergo hepatogenic differentiation. However, in previous experiments with four weeks administration of BM-MSCs in CCl<sub>4</sub>-treated mice, only a small precentage of MSCs underwent hepatocyte-like differentiation<sup>24</sup>.

At the molecular level, the transplantation of ASCs dysplayed significant effects on some of the key aspects of APAP-induced liver injury, and in particular on oxidative stress and JNK signaling. Oxidative stress is due to an imbalance beetwen ROS production and endogenous antioxidant defenses level and plays a pivote role in APAP-induced liver injury<sup>16-19</sup>. Moreover, it has been demonstrated that also nitrogen species, particular peroxynitrite, play a key role in APAP liver injury especially through DNA fragmentation<sup>16-19</sup>. In rats transplanted with ASCs,

we did not observe increased levels of isoprostanes, a marker of lipid peroxidation, neither of 8-OHG, a marker of DNA damage, indicating that ASCs protects from APAP-induced oxidative stress. Consistently, ASCs transplantation decreased nitrite/nitrates, which are sensitive markers of nitrosative stress, to the levels observed in healthy controls.

Finally, in recent years it has been demonstrated that JNK plays a key role in the pathogenesis of APAP-related liver injury<sup>20-22</sup>. Hepatic JNK activation preceded the onset of hepatocyte death both in human and murine paracetamol hepatotoxicity<sup>20-22</sup>. JNK inhibition in vivo, using different JNK inhibitors, markedly reduced mortality in murine paracetamol hepatotoxicity, with a significant reduction in hepatic necrotic and apoptotic death<sup>20-22</sup>. JNK inhibition is not protective in acute carbon tetrachloride-mediated or anti-Fas antibody-mediated hepatic injury<sup>20</sup>, suggesting specificity for the role of JNK in APAP hepatotoxicity and thereby identifying JNK as an important therapeutic target in the treatment of acetaminophen hepatotoxicity. Interestingly, ASCs transplantation was able to completely restore JNK signaling to levels of healthy rats.

In conclusion, in this study we demonstrated for the first time that ASCs transplantation is effective in treating APAP-induced ALF and encephalopathy. ASCs engraft in the injured liver, where exerts potent antioxidant effects and

inhibits JNK activation. Further studies are warranted in order to elucidate additional molecular pathways involved in the therapeutic effect of ASCs transplantation in ALF. In our opinion, our findings provide a strong rationale for the potential use of ASCs in the clinical management of patients with ALF.

## REFERENCES

1. Pittenger MF, Mackay AM, Beck SC et al. Multilineage potential of adult human mesenchymal stem cells. *Science* 1999;284:143–147.
2. Bieback K, Kern S, Kluter H, Eichler H. Critical parameters for the isolation of mesenchymal stem cells from umbilical cord blood. *Stem Cells* 2004;22:625– 634.
3. De Coppi P, Bartsch G Jr., Siddiqui MM et al. Isolation of amniotic stem cell lines with potential for therapy. *Nat Biotechnol* 2006;25:100 –106.
4. In't Anker PS, Scherjon SA, Kleijburg-van der Keur C et al. Isolation of mesenchymal stem cells of fetal or maternal origin from human placenta. *Stem Cells* 2004;22:1338 –1345.
5. Zuk PA, Zhu M, Mizuno H et al. Multilineage cells from human adipose tissue: Implications for cell-based therapies. *Tissue Eng* 2001;7:211–228.
6. Zuk PA, Zhu M, Ashjian P et al. Human adipose tissue is a source of multipotent stem cells. *Mol Biol Cell* 2002;13:4279–4295.
7. Schaffler A, Buchler C. Concise Review: Adipose tissue-derived stromal cells—Basic and clinical implications for novel cell-based therapies. *Stem Cells* 2007;25:818–827.

8. Ferrari G, Cusella-DeAngelis G, Coletta M, Paolucci E, Stornaiuolo A, Cossu G, et al. Muscle regeneration by bone marrow-derived myogenic progenitors. *Science* 1998;279:1528-1530.
9. Sanchez-Ramos J, Song S, Cardozo-Pelaez F, Hazzi C, Stedeford T, Willing A, et al. Adult bone marrow stromal cells differentiate into neural cells in vitro. *Exp Neurol* 2000;164:247-256.
10. Schwartz RE, Reyes M, Koodie L, Jiang Y, Blackstad M, Lund T, et al. Multipotent adult progenitor cells from bone marrow differentiate into functional hepatocyte-like cells. *J Clin Invest* 2002;109:1291-1302.
11. Sato Y, Araki H, Kato J, Nakamura K, Kawano Y, Kobune M, et al. Human mesenchymal stem cells xenografted directly to rat liver are differentiated into human hepatocytes without fusion. *Blood* 2005;106:756-763.
12. Kern S, Eichler H, Stoeve J, Kluter H, Bieback K. Comparative analysis of mesenchymal stem cells from bone marrow, umbilical cord blood or adipose tissue. *Stem Cells* 2006;24:1294-1301.
13. Seo MJ, Suh SY, Bae YC & Jung JS (2005) Differentiation of human adipose stromal cells into hepatic lineage in vitro and in vivo. *Biochem Biophys Res Commun* 328, 258–264.

14. Banas A, Teratani T, Yamamoto Y, Tokuhara M, Takeshita F, Quinn G, Okochi H & Ochiya T (2007) Adipose tissue-derived mesenchymal stem cells as a source of human hepatocytes. *Hepatology* 46, 219–228.
15. Bernal W, Auzinger G, Dhawan A, Wendon J. Acute liver failure. *Lancet*. 2010 Jul 17;376(9736):190-201.
16. Das J, Ghosh J, Manna P, Sil PC. Acetaminophen induced acute liver failure via oxidative stress and JNK activation: protective role of taurine by the suppression of cytochrome P450 2E1. *Free Radic Res*. 2010 Mar;44(3):340-55.
17. Cover C, Mansouri A, Knight TR, Bajt ML, Lemasters JJ, Pessayre D, et al. Peroxynitrite-induced mitochondrial and endonuclease-mediated nuclear DNA damage in acetaminophen hepatotoxicity. *J Pharmacol Exp Ther* 2005;315:879-887.
18. Knight TR, Ho YS, Farhood A, Jaeschke H. Peroxynitrite is a critical mediator of acetaminophen hepatotoxicity in murine livers: protection by glutathione. *J Pharmacol Exper Ther* 2002;303:468-475.
19. James LP, McCullough SS, Lamps LW, Hinson JA. Effect of N-acetylcysteine on acetaminophen toxicity in mice: relationship to reactive nitrogen and cytokine formation. *Toxicol Sci* 2003;75:458-467.

20. Gunawan BK, Liu ZX, Han D, Hanawa N, Gaarde WA, Kaplowitz N. c-Jun N-terminal kinase plays a major role in murine acetaminophen hepatotoxicity. *Gastroenterology* 2006; 131: 165-178
21. Henderson NC, Pollock KJ, Frew J, Mackinnon AC, Flavell RA, Davis RJ, Sethi T, Simpson KJ. Critical role of c-jun (NH2) terminal kinase in paracetamol- induced acute liver failure. *Gut* 2007; 56: 982-990
22. Arjunolic acid, a triterpenoid saponin, prevents acetaminophen (APAP)-induced liver and hepatocyte injury via the inhibition of APAP bioactivation and JNK-mediated mitochondrial protection. *Free Radic Biol Med.* 2010 Feb 15;48(4):535-53.
23. Soltys KA, Soto-Gutiérrez A, Nagaya M, et al. Barriers to the successful treatment of liver disease by hepatocyte transplantation. *J Hepatol.* 2010 Oct;53(4):769-74.
24. Kuo TK, Hung SP, Chuang CH, et al. Stem cell therapy for liver disease: parameters governing the success of using bone marrow mesenchymal stem cells. *Gastroenterology.* 2008 Jun;134(7):2111-21

25. Zemel R, Bachmetov L, Ad-El D, Abraham A, Tur-Kaspa R. Expression of liver-specific markers in naïve adipose-derived mesenchymal stem cells. *Liver Int.* 2009 Oct;29(9):1326-37.
26. Yin H, Cheng L, Holt M, et al. Lactoferrin protects against acetaminophen-induced liver injury in mice. *Hepatology* 2010;51(3):1007-16.
27. Ito Y, Bethea NW, Abril ER, McCuskey RS. Early hepatic microvascular injury in response to acetaminophen toxicity. *Microcirculation* 2003;10:391-400.
28. McCuskey RS. Sinusoidal endothelial cells as an early target for hepatic toxicants. *Clin Hemorheol Microcirc* 2006;34:5-10.
29. Williams AM, Langley PG, Osei-Hwediah J, Wendon JA, Hughes RD. Hyaluronic acid and endothelial damage due to paracetamol-induced hepatotoxicity. *Liver Int* 2003;23:110-115.
30. Banas A, Teratani T, Yamamoto Y, Tokuhara M, et al. IFATS collection: in vivo therapeutic potential of human adipose tissue mesenchymal stem cells after transplantation into mice with liver injury. *Stem Cells.* 2008 Oct;26(10):2705-12.